

# Inclusion of covalency effect in high pressure structural properties of some semiconducting ternary alloys

S. SINGH, P. BHARDWAJ\*

*Department of Physics, Barkatullah University, Bhopal-462026, India.*

We have investigated the phase transition pressures and associated volume collapses in the calcium chalcogenide mixed crystals using two models. A modified interaction potential model (model-I) has been developed by including covalency effect in interaction potential model (model-II) and the results from model-I are found to be better and they are in good agreement with experiment. The study has been extended to mixed crystals and the effect of composition on transition pressure, volume change, Cauchy violation and elastic anisotropy are investigated. To further enhance the reliability of present model and to judge the mechanical stability of present materials, elastic combinations, elastic wave velocity and average wave velocity are also calculated and effect of pressure on them is discussed. As the Poisson ratio is an important value to know the properties of compounds found in Earth's crust, we have calculated the Poisson ratio ( $\sigma$ ) of present chalcogenides and they are found to be in the range of  $\sim (0.22-0.25)$ .

(Received September 24, 2010; accepted November 19, 2010)

*Keywords:* Alloys, Semiconductors, High pressure, Crystal structure, Mechanical properties

## 1. Introduction

Structural B1-B2 phase transitions in II-IV compounds have been studied by many investigators, but the light and middle AX compounds ( $A = \text{Ca, Be, Mg}$ ) have not been systematically investigated. Among them IIA-VIA Calcium chalcogenides with high cation and anion ratio resulting in high phase transition pressures seem to be more challenging. The x-ray diffraction (XRD) reveals the first-order phase transition from the NaCl (B1) to CsCl (B2) [1] in these chalcogenides. To explore interesting features exhibited by the high pressure phase transition and pressure-volume relations in these CaX compounds, several efforts have been devoted using the full potential linearized APW [2], *ab initio* [3], pseudopotential [4,5] and tight binding [6] theories. The behaviour of these compounds having a cubic structure of the rock salt type was investigated by X-ray diffraction measurement at room temperature upto 52 GPa [1,2,7].

The significantly small volume collapse in CaSe and CaTe has been ascribed to the large disparity in their ionic radii among the heavy alkaline earth chalcogenides and hence the repulsive force between the large ions (anions) resist volume collapse at the phase transition in CaSe and CaTe as remarked by Luo et al [1]. Among these compounds CaS being an excellent luminescent material, has been considered to be an excellent host material for efficient cathode-ray tube phosphors [8]. Looking at the interesting properties of CaX, the knowledge of their structural stability and elastic behavior is very important from a device application point of view.

In the last two decades, some theoretical and experimental works have yielded information on aspects of the structural properties [1,3 9-13] and the electronic properties [14-17] of CaX. First principle density

functional theory and microscopic tight binding models as well as effective Hamiltonian models have been used successfully to address the electronic magnetic and structural ground state properties. On the other hand phenomenological lattice models [18-20] have proved very successful in obtaining a qualitative and quantitative understating with proper parameterization. Despite their success, the basic nature of these interatomic potentials is such that they are inadequate to reveal a realistic picture of the interaction mechanism in ionic solids. Marinelli et al [16] studied elastic constants and electronic structure of these chalcogenides with comparative study of performance of various Hamiltonians. Recently Slimani et al [17] extended their study to Calcium chalcogenide alloys and studied these alloys for structural properties and dependence of composition on bond strengthening or weakening effects. Wealth of data is available on experimental and theoretical front on CaX, but less attention is paid to the elastic constants and their behavior under pressure. So, a detailed work in structural properties and elastic behaviour under pressure in these chalcogenides is required. Looking at the interesting properties of CaX and the success of Slimani et al and the fact that the knowledge of structural stability and elastic property under pressure is very important, we have applied an effective and modified potential model to these chalcogenides and studied them under high pressure ( $\sim 80$  GPa) for different compositions.

It is seen from the current literature that three body potential model (TBP) used and developed by Singh and coworkers [18-21] has been found to be remarkably successful in giving the unified description of the lattice dynamic, static elastic, optic, dielectric and photo elastic properties of ionic and semi conducting crystals. In this TBP model, the three body interactions owe their origin to

the quantum mechanical foundation and also to the phenomenological approach [22-24] in terms of the transfer (or exchange) of charge between the overlapping electron shells of the adjacent ions in solids. This TBP approach [18] has been extended to include the Hafemeister-Flygare (HF) type [25] overlap repulsion operative upto the second neighbour ions for describing the lattice static and mechanical properties of binary ionic solids and alloys. Also, Tosi and coworkers [24] have demonstrated the significance of van der Waals (vdW) attraction due to the dipole-dipole (d-d) and dipole-quadruple (d-q) interactions to describe the cohesion in ionic solids and they are generally ignored in the first principle calculations. Besides, it is noted that Motida [26] has incorporated the effect of covalency to reveal the cohesive and lattice properties of partially covalent crystals.

Motivated from the above mentioned success of the TBP model in III-V and II-VI compound semiconductor, we thought it pertinent to apply a modified potential model for the prediction of phase transition pressures and associated volume collapses in CaX mixed compounds. In the present paper we have used two models, modified interaction potential model (MIPM) model-I (including covalency effect) and model-II (without including covalency effect) to study the effect of covalency on relative stability; phase transition pressure and elastic properties for B1 phase. As the present compounds are highly ionic and partially covalent semiconductors, it would be appropriate to include covalency effects in the potential model. Under high pressure these compounds transform to close packed structures. This effect is important in the study of structural phase transition in the present partially covalent compounds. The inclusion of covalency effects has improved the results on phase transition (B1-B2), elastic constants, combinations of elastic constants. The objective of present work is to investigate systematics of elasticity and thermodynamic properties and phase transition of calcium chalcogenide (CaX) mixed crystal. The chief aim of these potentials is a critical assessment of the performance of these two potentials in the study of phase transition and high pressure behavior of mixed CaX. The essential theory and method are described in the next section. The computed results are presented and discussed in the section 3.

## 2. Essentials of theory and computational method

The natural consequence of application of pressure on the crystals is the compression, which in turn leads to an increased charge transfer (or three-body interaction effects) [18-21] due to the existence of the deformed (or exchanged) charge between the overlapping electron shells of the adjacent ions.

These effects have been incorporated in the Gibbs free energy ( $G = U + PV - TS$ ) as a function of pressure and three body interactions (TBI), which are the most dominant among the many body interactions. Here,  $U$  is the internal energy of the system equivalent to the lattice energy at

temperature near zero and  $S$  is the entropy. At temperature  $T=0K$  and pressure ( $P$ ) the

$$G_{BX}(r) = \frac{-\alpha_M^X Z^2 e^2}{r} - \frac{12\alpha_M^X Z e^2 f_m(r)}{r} - \left[ \frac{C^X}{r^6} + \frac{D^X}{r^8} \right] + 6b\beta_{ij} \exp[(r_i + r_j - r^X)/\rho] + 6b\beta_{ij} \exp[(2r_j - Y_X r^X)/\rho] + 6b\beta_{jj} \exp[(2r_j - Y_X r^X)/\rho] + PV_{BX}(r^X) \quad (1)$$

Where  $X=1$  (Phase 1=B1), 2(Phase 2=B2), and  $Y_X=1.414, 1.154$ , for NaCl and CsCl structures respectively.

With  $\alpha_m^X$  (Where  $X=1$  (Phase 1=B1), 2(Phase 2=B2)) as the Madelung constant.  $C$  and  $D$  are the overall vander Waal coefficients for NaCl and CsCl structure respectively,  $\beta_{ij}$  ( $i, j=1, 2$ ) are the Pauling coefficients defined as  $\beta_{ij}=1+(Z_i/n_i)+(Z_j/n_j)$  with  $Z_i$  ( $Z_j$ ) and  $n_i$  ( $n_j$ ) as the valence and the number of electrons of the  $i(j)^{th}$  ion.  $Z$  is the ionic charge and  $b$  ( $\rho$ ) are the hardness (range) parameters,  $r$  is the nearest neighbour separations  $f_m(r)$  is the modified three body force parameter which includes the covalency effect with three body interaction,  $r_i$  ( $r_j$ ) are the ionic radii of ions  $i$  ( $j$ ).

These lattice energies consist of long range Coulomb energy (first term), three body interactions corresponding to the nearest neighbour separation  $r$  (second term), vdW (vander Waal) interaction (third term), energy due to the overlap repulsion represented by Hafemeister and Flygare (HF) type potential and extended up to the second neighbour ions (fourth, fifth and sixth terms).

Covalency effects have been included in the second terms of lattice energies given by Equation (1) in three-body interaction parameter on the lines of Motida [26]. Now modified three body parameter  $f_m(r)$  becomes

$$f_m(r) = f_{TBI}(r) + f_{cov}(r) \quad (2)$$

The relevant expressions of  $f_{cov}(r)$  are given in our earlier work [27].

The Gibb's free energies contain three model parameters [ $b$ ,  $\rho$ ,  $f_m(r)$ ], namely hardness, range and modified three body force parameter. The values of these parameters have been evaluated using the lattice energy and its first and second order space derivatives [19,21,27]:

$$\left[ \frac{dU}{dr} \right]_{r=r_0} = 0 \quad (3)$$

$$\frac{d^2U}{dr^2} = 9Kr_0B \quad (4)$$

The mixed crystals, according to the virtual crystal approximation (VCA) [28], are regarded as an array of average ions whose masses, force constants, and effective charges are considered to scale linearly with concentration ( $x$ ). The measured data on lattice constants in  $Ba_{1-x}Sr_xTe$  have shown that they vary linearly with the composition ( $x$ ), and hence they follow Vegards law [29]:

$$a(A B_{1-x} C_x) = (1-x)a(AB) + xa(AC) \quad (5)$$

The values of these model parameters are the same for end point members. The values of these parameters for their mixed crystal components have been determined from the application of Vegards law to the corresponding measured data for AB and AC. It is instructive to point that the mixed crystals, according to the virtual crystal approximation, are regarded as an array of average ions whose masses, force constants and effective charges are considered to scale linearly with concentration. It is convenient to find the three parameters for both binary compounds. Furthermore, we assume that these parameters vary linearly with  $x$  and hence follow Vegards law [29]:

$$b(A B_{1-x} C_x) = (1-x)b(AB) + xb(AC) \quad (6)$$

$$\rho(A B_{1-x} C_x) = (1-x)\rho(AB) + x\rho(AC) \quad (7)$$

$$f_m(r)(A B_{1-x} C_x) = (1-x)f_m(r)(AB) + xf_m(r)(AC) \quad (8)$$

### 2.1 Phase transition pressures

As, the stable phase is associated with minimum free energy of the crystal, we have followed the technique of minimization of Gibbs free energies of real and

$$C_{11} = (e^2 / 4a^4)[-5.112Z(Z + 12f_m(r)) + A_1 + (A_2 + B_2) / 2 + 9.3204zaf'_m(r)] \quad (9)$$

$$C_{12} = (e^2 / 4a^4)[0.226Z(Z + 12f_m(r)) - B_1 + (A_2 - 5B_2) / 4 + 9.3204zaf'_m(r)] \quad (10)$$

$$C_{44} = (e^2 / 4a^4)[2.556Z(Z + 12f_m(r)) - B_1 + (A_2 + 3B_2) / 4] \quad (11)$$

The values of  $A_i$ ,  $B_i$ , and  $C_i$  ( $i = 1, 2$ ) have been evaluated from the knowledge of  $b$ ,  $\rho$  and  $f_m(r)$  are given in our earlier work [27]:

### 2.3 Thermo physical properties

In order to assess the relative merit of the present potential and logarithmic potential (LP) [27], we have calculated the molecular force constant ( $f$ ), infrared absorption frequency ( $\nu_0$ ), Debye temperature ( $\theta_D$ ), Grunneisen parameter ( $\gamma$ ) and ratio of volume expansion coefficient ( $\alpha_v$ ) to specific heat ( $C_v$ ) at constant volume which are directly derived from the lattice energy,  $U(r)$ .

The compressibility is well known to be given by

$$\beta = \frac{3Kr_0}{f} \quad (12)$$

in terms of molecular force constants

$$f = \frac{1}{3} \left[ U_{kk'}^{SR}(r) + \frac{2}{r} U_{kk'}^{SR}(r) \right]_{r=r_0} \quad (13)$$

With  $U_{kk'}^{SR}(r)$  as the short range nearest neighbour ( $K \neq K'$ ) part of  $U(r)$  given by the last three terms in Equation (1). This force constant  $f$  leads to the infrared absorption frequency with the knowledge of the reduced mass ( $\mu$ ) of the crystals.

hypothetical phases. We have minimized  $G_{B1}(r)$  and  $G_{B2}(r')$  given by Equation (1) at different pressures in order to obtain the interionic separations  $r$  and  $r'$  corresponding to B1 and B2 phases associated with minimum energies. The phase transition occurs when  $\Delta G$  approaches zero and associated pressure is phase transition pressure ( $P_t$ ). Up to  $P_t$  the compound is stable under B1 structure while at  $P_t$  theoretically we can say both the phases (B1 and B2) coexist, after which system becomes stable under B2 structure. At  $P_t$  these compounds undergo a (B1-B2) transition associated with a sudden change in volume showing a first order phase transition.

### 2.2 Elastic properties

The present model (MIPM) for the NaCl and CsCl phases contains three model parameters ( $b$ ,  $\rho$ ,  $f_m(r)$ ), using them the elastic constants [27] have been computed. The expressions of elastic constants are as follows:

$$\nu_0 = \frac{1}{2\pi} \left( \frac{f}{\mu} \right)^{1/2} \quad (14)$$

This frequency gives us the Debye temperature

$$\theta_D = \frac{h\nu_0}{k} \quad (15)$$

With  $h$  and  $k$  as the Planck and Boltzman constants, respectively.

The values of the Grunneisen parameter ( $\gamma$ ), have been calculated from the relation

$$\gamma = -\frac{r_0}{6} \left[ \frac{U'''(r)}{U''(r)} \right]_{r=r_0} \quad (16)$$

We have calculated the ratio of the volume expansion coefficient ( $\alpha_v$ ) to the volume to specific heat ( $C_v$ ) from its well known expression

$$\frac{\alpha_v}{C_v} = -\left[ \frac{U'''(r)}{2rU''(r)} \right]_{r=r_0} \quad (17)$$

The thermal expansion coefficient ( $\alpha_v$ ) can be calculated with the knowledge of specific heat ( $C_v$ ).

### 3. Results and discussion

Using these model parameters and the minimization technique phase transition pressures of perfect and mixed calcium chalcogenides have been computed. The input data of the crystal and calculated model parameters are listed in Table-1. In order to obtain the structural phase transition, we have followed the technique of minimization. By minimizing  $U_{B1}(r)$  and  $U_{B2}(r')$  at different pressures we obtained the interionic separations  $r$  and  $r'$  associated with minimum energies for  $B_1$  and  $B_2$  phases, respectively. We have evaluated the corresponding  $G_{B1}(r)$  and  $G_{B2}(r')$  and their respective differences  $\Delta G (= G_{B1}(r) - G_{B2}(r'))$ .

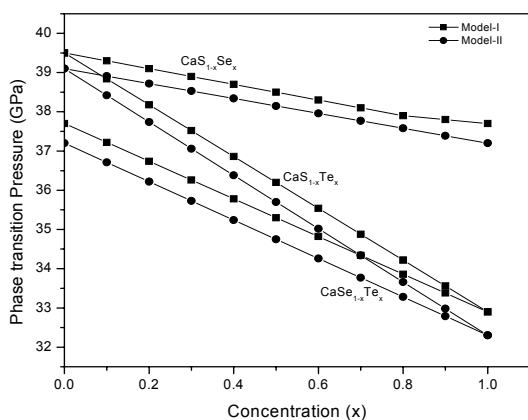


Fig. 1. Variation of phase transition pressure with concentration (x) of CaX compounds, solid squares (■), solid circles (●) and solid triangles (▲) represent model-I for  $CaS_{1-x}Se_x$ ,  $CaSe_{1-x}Te_x$  and  $CaS_{1-x}Te_x$  respectively. The solids lines represent model-II for  $CaS_{1-x}Se_x$ ,  $CaSe_{1-x}Te_x$  and  $CaS_{1-x}Te_x$  respectively.

Table 1. Input parameters and generated model parameters for calcium chalcogenides.

Compounds	Input Parameters		Model Parameters		
	$r_0$ (Å)	B (GPa)	$b(10^{-12}$ ergs)	$\rho$ (Å)	$f_m(r)$
CaS	2.84 <sup>a</sup>	64 <sup>a</sup>	0.321	0.295	- 0.201
CaSe	2.96 <sup>a</sup>	51 <sup>a</sup>	0.873	0.385	- 0.411
CaTe	3.17 <sup>a</sup>	42 <sup>a</sup>	0.279	0.389	- 0.602

ref-a-[1]

As the pressure is increased the value of  $\Delta G$  decreases and approaches zero at the transition pressure. Beyond this pressure  $\Delta G$  becomes negative as the phase  $B_2$  becomes stable. The calculated phase transition pressure for CaX are

listed in Table-2 and plotted in Fig. 1. The phase transition pressure of CaX are dependent linearly with concentration (x). Fig.1 shows our present computed phase transition pressure with concentration for  $CaS_{1-x}Se_x$ ,  $CaSe_{1-x}Te_x$  and  $CaS_{1-x}Te_x$  respectively. The values of phase transition pressures of CaX mixed crystals for model-I and model-II at different concentrations are compared with experimental and others data in Table-2. The first order phase transition involving a discontinuity in volume takes place at the transition pressure. Experimentally one usually studies the relative volume changes ( $-\Delta V/V_0$ ) associated with the compressions. The discontinuity in volume ( $-\Delta V/V_0$ ) at the transition pressure is obtained from the phase diagram. This is the characteristic of first order phase transition. The negative sign shows compression in crystal. The relative volume change of mixed CaX crystals are also given in Table-2 and they are plotted in Fig-2. We have also computed the relative volume changes  $V(P)/V(0)$  corresponding to the values of  $r$  and  $r'$  at different pressures. It is clear from Table 2 that our calculated volume collapses  $-\Delta V_{(p)}/V_{(0)}$  from our modified model for CaS, CaSe and CaTe are 9.8%, 7.2% and 4.3% respectively which are close to the results reported by Cortona et al [3] and they are slightly better matching with available experimental results [1] than Cortona et. al. The  $-ve$  sign shows the compression in crystal. The values of model-I and model-II of end point members are compared with experimental and other theoretical data. It is clear from Table-2 and Fig-2 that our values of model-I are better matching with experimental values than other theoretical values though the difference is small but improvement is towards accuracy. The values of volume collapses of CaX mixed crystals at different concentrations are compared with pseudoexperimental data (calculated by applying Vegard's law to experimental values).

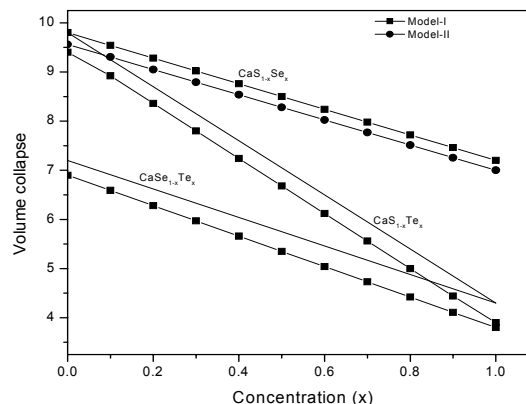


Fig. 2. Variation of volume collapse with concentration of CaX compounds solid squares (■) represents model-I for  $CaS_{1-x}Se_x$ ,  $CaSe_{1-x}Te_x$  and  $CaS_{1-x}Te_x$  respectively. The solid lines represent model-II  $CaS_{1-x}Se_x$ ,  $CaSe_{1-x}Te_x$  and  $CaS_{1-x}Te_x$  respectively.

Table-2 Phase transition and volume collapse of CaX at different concentration.

Alloys/ Concentration	Phase Transition Pressure (GPa)				Volume Collapse (%)			
	Present		Expt.	Others	Present		Expt.	Others
	Model-I	Model-II			Model-I	Model-II		
CaS <sub>1-x</sub> Se <sub>x</sub> 0	39.5	39.1	40.0 <sup>a</sup>	37.22 <sup>b</sup>	9.8	9.56	10.2 <sup>a</sup>	7.7 <sup>c</sup>
0.25	39.04	38.62	39.5 <sup>a</sup>	36.5 <sup>b</sup>	9.15	8.92	9.58 <sup>a</sup>	7.55 <sup>c</sup>
0.5	38.6	38.15	39 <sup>a</sup>	35.8 <sup>b</sup>	8.5	8.28	8.96 <sup>a</sup>	7.4 <sup>c</sup>
0.75	38.14	37.67	38.5 <sup>a</sup>	35.09 <sup>b</sup>	7.85	7.64	8.34 <sup>a</sup>	7.25 <sup>c</sup>
1	37.7	37.20	38.0 <sup>a</sup>	34.38 <sup>b</sup>	7.2	7.0	7.7 <sup>a</sup>	7.1 <sup>c</sup>
CaSe <sub>1-x</sub> Te <sub>x</sub> 0	37.7	37.2	38.0 <sup>a</sup>	34.38 <sup>b</sup>	7.2	6.9	7.7 <sup>a</sup>	7.1 <sup>c</sup>
0.25	36.49	35.975	36.7 <sup>a</sup>	33.38 <sup>b</sup>	6.47	6.12	6.93 <sup>a</sup>	6.85 <sup>c</sup>
0.5	35.33	34.75	35.5 <sup>a</sup>	32.39 <sup>b</sup>	5.75	5.35	6.16 <sup>a</sup>	6.6 <sup>c</sup>
0.75	34.10	33.52	34.2 <sup>a</sup>	31.40 <sup>b</sup>	5.02	4.57	5.39 <sup>a</sup>	6.35 <sup>c</sup>
1	32.9	32.3	33.0 <sup>a</sup>	30.41 <sup>b</sup>	4.3	3.8	4.6 <sup>a</sup>	6.1 <sup>c</sup>
CaS <sub>1-x</sub> Te <sub>x</sub> 0	39.5	39.1	40.0 <sup>a</sup>	38.0 <sup>b</sup>	9.8	9.3	10.2 <sup>a</sup>	7.7 <sup>c</sup>
0.25	37.85	37.39	38.2 <sup>a</sup>	36.11 <sup>b</sup>	8.42	7.95	8.8 <sup>a</sup>	7.3 <sup>c</sup>
0.5	36.2	35.7	36.5 <sup>a</sup>	34.22 <sup>b</sup>	7.05	6.6	7.4 <sup>a</sup>	6.9 <sup>c</sup>
0.75	34.55	34.0	34.7 <sup>a</sup>	32.33 <sup>b</sup>	5.67	5.25	6.0 <sup>a</sup>	6.5 <sup>c</sup>
1	32.9	32.3	33.0 <sup>a</sup>	30.41 <sup>a</sup>	4.3	3.9	4.6 <sup>a</sup>	6.1 <sup>c</sup>

a-ref [1], b-ref [2], c-ref [3]

To test the mechanical stability of our model, we have computed the elastic properties of proposed materials. Also, we could reproduce the correct sign of the elastic constants ( $C_{11}$ - $C_{12}$ ) and  $C_{44}$ . The elastic constant  $C_{11}$  represents elasticity in length. A longitudinal strain produces a change in  $C_{11}$ . The elastic constants  $C_{12}$  and  $C_{44}$  are related to the elasticity in shape, which is a shear constant. A transverse strain causes a change in shape without a change in volume. Therefore,  $C_{12}$  and  $C_{44}$  are less sensitive of pressure as compared to  $C_{11}$ .

To study the elastic behavior of calcium compounds we have studied second order elastic constants (SOECs) and their combinations. We have made further investigations from the variations of the bulk modulus  $B = (C_{11} + 2C_{12})/3$ , the combination of SOEC: elastic stiffness  $C_L = (C_{11} + C_{12} + 2C_{44})/2$  and the shear moduli  $C_s = (C_{11} - C_{12})/2$ . The values of these combinations for model-I and model-II are given in Table-3 at  $P=0$  GPa.

Table 3. Elastic combinations at  $P=0$  GPa of CaX at different concentration.

Compounds	CaS		CaSe		CaTe	
	Model-I	Model-II	Model-I	Model-II	Model-I	Model-II
Bulk modulus (B) (GPa)	62.36	61.87	50.45	51.39	39.67	43.17
Shear modulus (G) (GPa)	38.38	36.92	31.47	34.93	26.22	28.25
Elastic stiffness ( $C_L$ )	114.24	112.83	91.35	93.47	70.96	72.32
Elastic anisotropy (A)	1.0853	1.0635	0.8228	0.8122	0.5059	0.5313
Cauchy violation ( $\delta$ ) (GPa)	-1.71	-1.78	-2.24	-2.61	-4.04	-3.92

We have also calculated the lattice constant (a) and bulk modulus (B) for perfect and mixed calcium chalcogenides at different concentrations. The computed values of lattice constants and bulk modulus for both the models are given in Table-4. The composition dependence of the bulk modulus and lattice constant for the alloys

under investigation is compared with the result of FP-LAPW. It is clear from Table-4 that our results for model-I are close with the values of Slimani et al [17] than model-II. It is clearly seen that the bulk modulus decreases by increasing the chalcogenide atomic number.

Table 4. Lattice constant and bulk modulus of CaX compounds at different concentration.

Alloys/ Concentration	Lattice constant a (Å)				Bulk modulus B (GPa)			
	Present		Expt.	Others	Present		Expt.	Others
	Model-I	Model-II			Model-I	Model-II		
CaS <sub>1-x</sub> Se <sub>x</sub> 0	5.80	5.44	5.689 <sup>a</sup>	5.722 <sup>b</sup>	62.360	61.87	51 <sup>a</sup>	47.958 <sup>b</sup>
0.25	5.855	5.485	-	5.787 <sup>b</sup>	59.382	59.25	-	49.910 <sup>b</sup>
0.5	5.91	5.53	-	5.847 <sup>b</sup>	56.405	56.631	-	52.499 <sup>b</sup>
0.75	5.965	5.575	-	5.906 <sup>b</sup>	53.427	54.009	-	55.176 <sup>b</sup>
1	6.02	5.62	5.916 <sup>a</sup>	5.964 <sup>b</sup>	50.453	51.39	64 <sup>a</sup>	57.106 <sup>b</sup>
CaSe <sub>1-x</sub> Te <sub>x</sub> 0	6.02	5.62	5.916 <sup>a</sup>	5.964 <sup>b</sup>	50.452	51.39	41.8 <sup>a</sup>	47.958 <sup>b</sup>
0.25	6.04	5.675	-	6.088 <sup>b</sup>	47.754	49.334	-	43.806 <sup>b</sup>
0.5	6.06	5.73	-	6.022 <sup>b</sup>	45.062	47.28	-	41.453 <sup>b</sup>
0.75	6.08	5.785	-	6.303 <sup>b</sup>	42.365	45.389	-	40.256 <sup>b</sup>
1	6.10	5.84	6.348 <sup>a</sup>	6.396 <sup>b</sup>	3.67	43.17	51 <sup>a</sup>	38.724 <sup>b</sup>
CaS <sub>1-x</sub> Te <sub>x</sub> 0	5.80	5.44	5.689 <sup>a</sup>	5.722 <sup>b</sup>	62.36	61.87	64 <sup>a</sup>	57.106 <sup>b</sup>
0.25	5.875	5.54	-	5.920 <sup>b</sup>	56.687	57.194	-	50.055 <sup>b</sup>
0.5	5.950	5.64	-	6.099 <sup>b</sup>	50.85	52.52	-	43.613 <sup>b</sup>
0.75	6.025	5.74	-	6.258 <sup>b</sup>	45.342	47.84	-	41.122 <sup>b</sup>
1	6.10	5.84	6.348 <sup>a</sup>	6.396 <sup>b</sup>	39.67	43.17	41.8 <sup>a</sup>	38.724 <sup>b</sup>

ref-a-[1], b [17]

For the calculation of elastic moduli, models based on two body central forces necessarily fail to reproduce the measured deviation from the Cauchy inequality  $C_{12} \neq C_{44}$  for cubic crystals. At  $P=0$  we take Cauchy inequality  $C_{12} \neq C_{44}$  only. This inequality must hold for an unstressed lattice at its minimum energy configuration ( $P=0$ ) if the lattice energy is determined by strictly pairwise interactions between the component ions [30]. One common approach is to assume that the atoms are connected with springs and that the resulting forces are only in the direction of the nearest neighbors (central force model). The deviation from the Cauchy violation  $\delta = C_{12} - C_{44} - 2P$  is a measure of the contribution from the non central many-body force since the Cauchy violation  $C_{12} = C_{44} + 2P$  should be satisfied when interatomic potentials are purely central. Violations of the Cauchy condition require noncentral forces and therefore provide an important measure of many body interactions. As shown in Fig. 3 and 4 that  $C_{12} - C_{44} = -1.78$  GPa at zero pressure for CaS and becomes more negative with increasing pressure and this trend is same as reported by Shimizu et. al. [31]. Fig 3 shows the dependence of  $\delta/C_{12}$  with concentration ( $x$ ) for CaS<sub>1-x</sub>Se<sub>x</sub>, CaSe<sub>1-x</sub>Te<sub>x</sub> and CaS<sub>1-x</sub>Te<sub>x</sub> using model-I and model-II. The Cauchy violation  $\delta/C_{12}$  shows a linear dependence on concentration ( $x$ ).

In case of CaS we have studied the Cauchy violation with increasing pressures up to 70 GPa and plotted them in Fig-4 from model I and model-II.

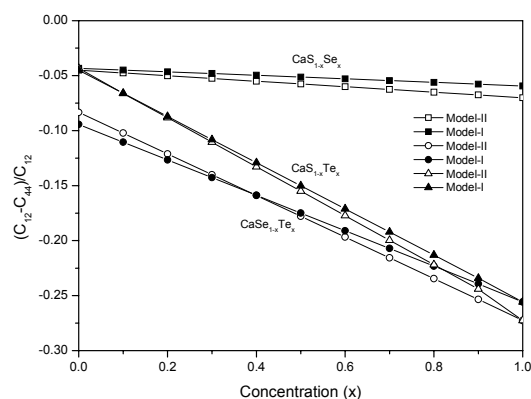


Fig. 3. Variation of Cauchy violation with concentration ( $x$ ) of CaX compounds. Solid squares solid circles and solid triangles with lines represent model- I and open squares, open circles and open triangles with lines represent model- II for CaS<sub>1-x</sub>Se<sub>x</sub>, CaSe<sub>1-x</sub>Te<sub>x</sub> and CaS<sub>1-x</sub>Te<sub>x</sub> respectively.

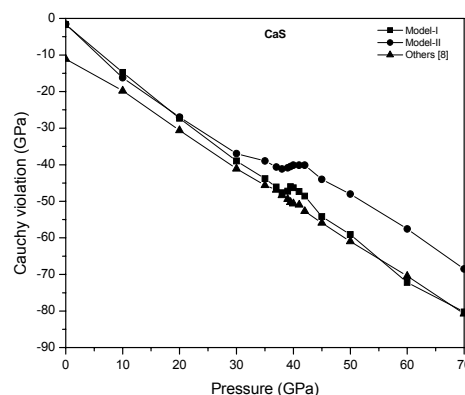


Fig. 4. Variation of Cauchy violation with pressure of CaS. Solid  $\blacksquare$ ,  $\bullet$  and  $\blacktriangle$  with lines represent model- I, model-II and others [8].

These results have been compared with first principle calculation results [8]. As pressure increases the calculated value of  $C_{12}-C_{44} = 2P$  decreases. Thus the degree of departure from the Cauchy condition is a measure of the non central or many body terms in the crystal potential. The deviation from the Cauchy condition is negative for the present compounds. The deviation  $\delta$  becomes larger as the pressure increases, which proves that the noncentral many body force becomes more and more important at high pressure. After phase transition pressure there is some deviation in model-II, but model-I shows almost same trend as reported by others [8]. Here, we can see that the inclusion of covalency effects in potential model (model-I) has improved the results. The values of Cauchy violation  $\delta$  are given in Table-3 at zero temperature and pressure.

Table 5. Normalized Elastic constants for CaX.

Normalized elastic constants	CaS		CaSe		CaTe	
	Model-I	Model-II	Model-I	Model-II	Model-I	Model-II
$C'_{11}$ (present) (Others)	1.7819 0 2.2451 0 <sup>a</sup>	1.792 8	1.934 3	1.923 9	2.252 8	2.242 8
$C'_{12}$ (present) (Others)	0.6090 4 0.4536 2 <sup>a</sup>	0.603 5	0.532 8	0.538 0	0.373 5	0.378 5
$C'_{44}$ (present) (Others)	0.6364 6 0.6284 5 <sup>a</sup>	0.632 4	0.577 2	0.587 8	0.475 3	0.475 3

a-ref [8]

It is known that even the cubic crystal which is isotropic structure, has elastic anisotropy as a result of a fourth rank tensor property of elasticity. The elastic anisotropic parameter of a cubic crystal is defined as [8].

$$A = \frac{2C_{44} + C_{12}}{C_{11}} - 1 \quad (18)$$

We have obtained the elastic anisotropic parameter A at various pressures and shown them in Fig-5. It is clear from Fig-5 that the anisotropy decreases when pressure increases, and our results agree with those reported by others [8]. The anisotropy factor drops rapidly with pressure and then decreases more slowly at higher pressures. The values of anisotropic parameter A at zero temperature and pressure are given in Table-3.

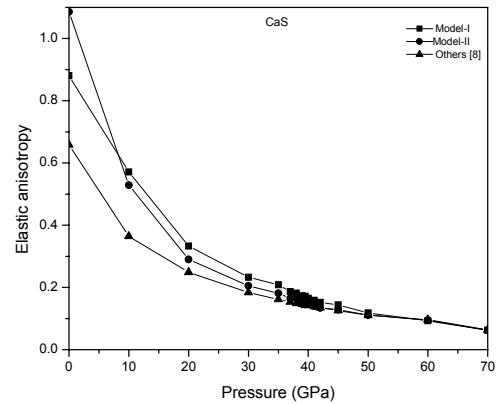


Fig. 5. Variation of elastic anisotropy with pressure of CaS. Solid ■, ● and ▲ with lines represent model- I, model-II and others [8].

To see the effect of anisotropic parameter A in mixed crystal system, we have plotted the anisotropic parameter A with concentration (x). The plot of  $CaS_{1-x}Se_x$ ,  $CaSe_{1-x}Te_x$  and  $CaS_{1-x}Te_x$  for model-I and Model-II are represented in Fig 6 (a-c) respectively. The elastic anisotropic parameter A varies linearly with concentration (x).

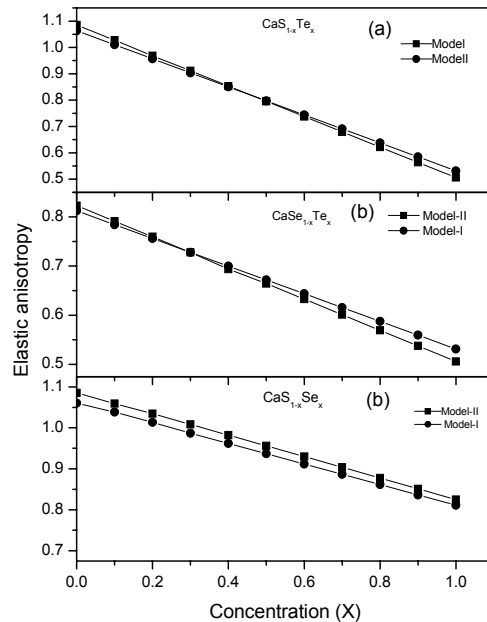


Fig. 6. Variation of Elastic anisotropy (A) with concentration (x) of CaX. solid circles (●) + lines represent model- I and the solid squares (■) + lines represent model-II  $CaS_{1-x}Se_x$ ,  $CaSe_{1-x}Te_x$  and  $CaS_{1-x}Te_x$  respectively.

Elastic properties under pressure are important to know the mechanical stability of material. To explore and investigate elasticity of CaX compounds under pressure, we have used normalized elastic constants  $c_{ij}$  [32]. The value of  $c_{ij}$  is obtained by dividing a specific elastic constant by the bulk modulus

$$c_{ij} = C_{ij}/B = 3C_{ij}/(C_{11} + 2C_{12}). \quad (19)$$

Dividing by the bulk modulus, the interatomic forces are normalized with an average restoring force of the system. We have extended the concept of the normalized elastic constant to the high pressure condition and  $c_{ij}$  for CaS as a function of pressure has been plotted in Fig 7. The Fig shows that all normalized elastic constants are decreasing slowly with increasing pressure. The values of  $c_{12}$  decrease slowly and the figure shows that the pressure dependence of  $c_{12}$  is almost linear. Comparing with  $c_{12}$  and  $c_{44}$  under pressure, only the values of  $c_{11}$  increase. The values of normalized elastic constants are given in Table-5 for CaS, CaSe and CaTe at zero temperature and pressure and they are comparable with the first principle calculations [8].

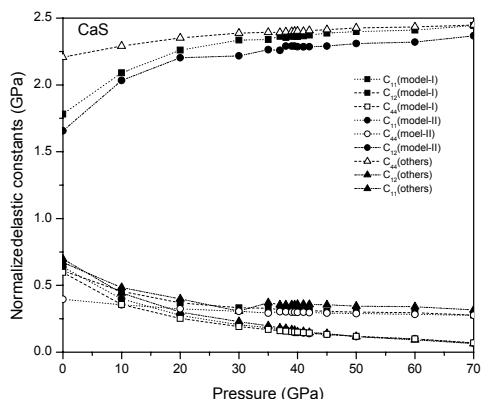


Fig. 7. The dependence of normalized elastic constants with pressure. Solid  $\blacksquare$ ,  $\bullet$  and  $\blacktriangle$  with lines represent model-I, model-II and others.

The well known Born stability criteria can be derived by expanding the internal energy in the strain and by requiring convexity of the energy of the energy. Three generally accepted elastic stability criteria for a cubic crystal are

$$C_{11} + 2C_{12} > 0 \quad C_{44} > 0 \quad C_{11} - C_{12} > 0 \quad (20)$$

For a cubic crystal under hydrostatic pressure, the generalized elastic stability criteria [32] in analogy to the conventional criteria (Equation (20)) are

$$c_{11} + 2c_{12} > 0 \quad c_{44} > 0 \quad c_{11} - c_{12} > 0 \quad (21)$$

In the case of hydrostatic pressure, the  $c_{ij}$  (in Voigt notation) are related to the  $C_{ij}$  defined with respect to the Eulerian strain variables by

$$c_{11} = C_{11} \quad c_{12} = C_{12} + P \quad c_{44} = C_{44} - P/2 \quad (22)$$

The finite-load stability conditions (Equation (21)) for a cubic crystal reduce to the Born stability criteria in the limit of vanishing load.

The elastic stiffness (in Voigt notation), are the appropriate elastic parameters which determine not only the acoustic velocities and Cauchy relations but also determine the stability of a crystal under hydrostatic pressure. Moreover, although only hydrostatic pressure is investigated here, the elastic stability criteria expressed in terms of the elastic stiffness coefficients should provide a generalization of the stability criteria valid under arbitrary stress [32-36].

In case of hydrostatic pressure  $P$ , to make comparison with experimental results, the elastic constants  $c_{ij}$  must be transformed into the observable elastic constants  $C_{ij}$  defined with respect to the finite strain variables [32-36].  $C_{ij}$  is transformed into  $c_{ij}$  (in Voigt notation) at hydrostatic compression as follows:

$$c_{11} = C_{11}, c_{12} = C_{12} + P, c_{44} = C_{44} - \frac{P}{2} \quad (23)$$

The shear modulus  $G$  can be defined by the following equation

$$G = (G_V + G_R) / 2 \quad (24)$$

Where

$$G_V = (2c + 3c_{44}) / 5$$

$$G_R = 15(6/c + 9/c_{44})^{-1}$$

and  $c = (c_{11} - c_{12}) / 2$

$G_V$  is the Voigt shear modulus and  $G_R$  is the Reuss shear modulus. Our calculated shear modulus  $G$  and bulk modulus  $B (=C_{11}+2C_{12})/3$  of these chalcogenides at zero pressure and zero temperature are listed in Table-3.

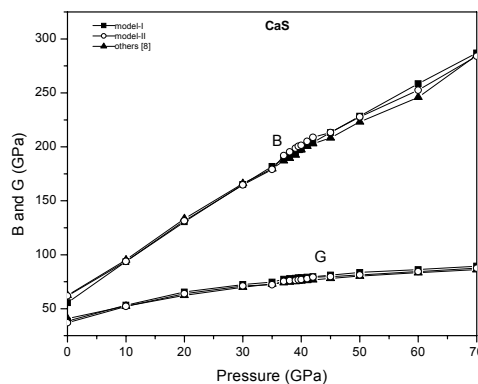


Fig. 8. Bulk and shear modulus of CaS as a function of pressure for CaS.

To see the effect of high pressure on Bulk and shear modulus, we have plotted them as a function of pressure in Fig 8 for CaS and compared them with the first principle calculations [8]. It is clear from this Fig that bulk modulus increases rapidly and shear modulus increase slowly with pressure. As the bulk modulus is inverse of compressibility ( $B=1/\beta$ ) i.e. compressibility decreases with pressure. Here we have included the wider pressure ranges than the pressure ranges where the B1 phase is stable.

The Poisson's ratio of a material influences the speed of propagation and reflection of stress waves. In geological applications, the ratio of compression to shear wave speed is important in inferring the nature of the rock deep in the Earth. In a geological timescale, excessive erosion or sedimentation of Earth's crust can either create or remove large vertical stresses upon the underlying rock. They deform in the horizontal direction as a result of

Poisson's effect. The expression of Poisson's ratio  $\sigma$  can be given in the following form:

$$\sigma = \frac{3B - 2G}{6B + 2G} \quad (25)$$

This ratio measures the extent of this effect in a particular substance. The Poisson's ratio has two limits: it must be greater than -1, and less than or equal to 0.5. The Poisson ratio for most metals falls between 0.25 to 0.35. The calculated values of Poisson ratio  $\sigma$  for CaS, CaSe and CaTe are given in Table-6. All these values are positive and lie between 0.22 to 0.25. In the structural view, the reason for the usual positive Poisson's ratio is that inter-atomic bonds realign with deformation.

Table 6. Elastic wave velocity and Poisson ratio for CaX.

Compounds	CaS		CaSe		CaTe	
	Model-I	Model-II	Model-I	Model-II	Model-I	Model-II
Longitudinal elastic wave velocity ( $V_l$ ) (m/s)	6607.5	6536.5	5905.2	6080.0	3914.6	4074.1
Transverse elastic wave velocity ( $V_t$ ) (m/s)	3841.8	3768.2	3446.0	3630.5	2320.3	2408.3
Poisson ratio ( $\sigma$ )	0.2446	0.2540	0.24179	0.22292	0.229188	0.231395

The variation of Poisson ratio  $\sigma$  with pressure for CaS for both the models along with first principle calculations are given in Fig 9. Poisson ratio  $\sigma$  increases with pressure up to the phase transition pressure. After phase transition pressure the value of Poisson ratio  $\sigma$  becomes almost constant with pressure. This may be because of the fact that after phase transition atoms takes a new place in a new arrangement leading to more compressed system.

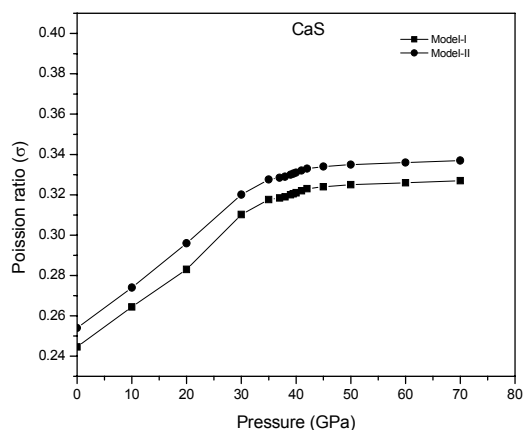


Fig. 9. Poisson ratio ( $\sigma$ ) of CaS as a function of pressure. The solid squares ( $\blacksquare$ ), solid circles ( $\bullet$ ) represent for model-I and model-II respectively.

The basic material properties, which are of interest in many manufacturing and research applications, can be determined quickly and easily through computations based on sound velocities. Sound velocity can be easily measured using ultrasonic pulse-echo techniques.

In addition, to study the thermodynamic properties of these compounds we have calculated the average wave velocity  $v_m$  on the lines of Yun-Dong Guo, et al [8]. For calculating the average wave velocity  $v_m$  the expressions is as follows:

$$v_m = \left[ \frac{1}{3} \left( \frac{2}{v_l^3} + \frac{1}{v_t^3} \right) \right]^{-1/3} \quad (26)$$

where  $v_l$  and  $v_t$  are the longitudinal and the transverse elastic wave velocities respectively, which are obtained from Navier's equation in the following forms:

$$v_l = \sqrt{\frac{3B + 4G}{3\rho}} \quad (27)$$

$$v_t = \sqrt{\frac{G}{\rho}} \quad (28)$$

where  $\rho$  is the density. The calculated values of longitudinal and transverse wave velocities are given in Table-6, using model-I and model-II. Due to the unavailability of the values of average wave velocities of CaX compounds, we could not compare our results. The average wave velocities of these chalcogenides are lying between  $1.8 \times 10^{10}$  and  $5.3 \times 10^{10}$  for both the models. We have plotted the longitudinal and transverse wave velocities as a function of pressure in Fig 10. It is clear from this Fig that the sound velocity increases with pressure.

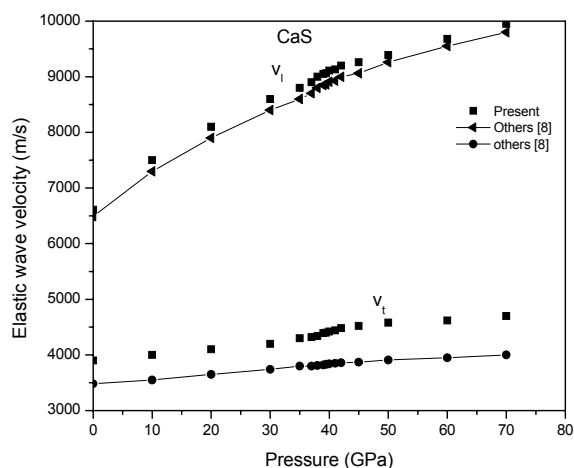


Fig. 10. The pressure dependence of elastic wave velocity  $v_l$  and  $v_t$  of CaS. Solid  $\blacksquare$ ,  $\bullet$  and  $\blacktriangle$  with lines represent present others (for  $v_l$ ) and others (for  $v_t$ ).

Besides we have calculated thermo physical properties of CaX. The thermo physical properties provide us the interesting information about the substance. The Debye characteristic temperature  $\theta_D$  reflects its structure stability, the strength of bonds between its separate elements, structure defects availability (dislocations in crystalline structure of mineral grains, pores, microcracks) and its density. Compressibility is used in the earth science to quantify the ability of a soil or rock to reduce in volume with applied pressure. These properties become important as the present compounds are found in earth crust. The calculated thermo physical properties have been listed in Table 7. Due to the lack of experimental data, we could not compare them with our results. Presently they are of only academic importance and may be used as a guide to experimentalists.

In view of the overall achievements, it may be concluded that in general there is reasonably good agreement of modified interionic potential model MIPM (Model-I) with the available experimental and theoretical values. The results from MIPM (model-I) are in general better matching with available data than the results of TBP (model-II). The success achieved in the present investigation can be ascribed to the realistic approach of our model, which reiterates the importance of inclusion of covalency effects. The charge transfer effect seems to be of great importance at high pressure when the inter-ionic separation reduces considerably and the coordination number increases. For the study of the phase transitions in partially covalent chalcogenides, we have incorporated, probably for the first time, the effect of covalency in the TBP model along with the vander Waals interactions for present compounds.

Table 7. Thermo physical properties of CaX.

Crystal	$f$ ( $10^4$ dyn/cm)	$\nu_0$ ( $10^{12}$ Hz)	$\theta_D$ (K)	$\gamma$	$\alpha_v/c_v$ ( $10^3$ J)
CaS	1.1938	3.7958	396.69	1.35	5.90
CaSe	1.4276	3.9432	454.21	1.29	4.35
CaTe	0.9867	2.9640	379.86	1.60	4.05

Finally, it may be concluded that the present modified interaction potential model (MIPM) is adequately suitable for describing the phase transition phenomena, elastic and thermophysical properties of these present chalcogenides and it has potential to study other structures also.

#### Acknowledgement

One of the authors (PB) is grateful to the Department of Science & Technology (DST), New Delhi for awarding WOS-'A' and the financial support to this work.

#### References

- [1] H. Luo, Raymond G. Greene, Kouros Ghandehari, Ting Li, A. L. Ruoff Phys. Rev. B **50**, 16232 (1994).
- [2] Z Charifi, H. Baaziz, F El Haj Hassan, N Bouarissa J Phys: Condens. Matter, **17**, 4083 (2005).
- [3] P. Cortona, P. Masi J Phys.: Condens. Matter, **10**, 8947 (1998).
- [4] F. Marinelli, A Lichanot Chem. Phys. Lett., **367**, 430 (2003).
- [5] S. Froyen, M.L Cohen, J. Phys. C **19**, 2623 (1983).

- [6] G K Straub, W A Harrison Phys. Rev. B **39**, 10325 (1989).
- [7] H. G. Zimmer., H. Winze, K. Syassen Phys. Rev. B **32**, 4066 (1985).
- [8] Yun-Dong Guo, Ze-Jin Yang, Qing-He Gao, Zi-Jiang Liu, Wei Dai, J Phys: Condens. Matter, **20**, 115203 (2008).
- [9] P E V Camp, V E V Doren, J L Martins, Phys. Status Solidi (b), **190**, 193 (1995).
- [10] S Ekbundit, A Chizmeshya, R La Violette, G H Wolf, J. Phys.: Condens. Matter, **8**, 8251 (1996).
- [11] R Pandey, J E Jaffè, A B Kunz, Phys. Rev. B **43**, 9228 (1991).
- [12] W Y Pa Ching, F Gan, M Z Huang, Phys. Rev. B **52**, 1596 (1995).
- [13] F El Haj Hassan, B Amrani J. Phys.: Condens. Matter, **19**, 386234 (2007).
- [14] P. Cortona, A V Monteleone, P Becker, Int. J. Quantum Chem., **56**, 831 (1995).
- [15] Z J Chen, H Y Xiao, X T Zu, Physica B **391**, 193 (2007).
- [16] F. and A. Lichanot, Chemical Phys. Lett. **367**, 430 (2003).
- [17] M. Slimani, H. Meradji, C. Sift, S. Labdi, S. Ghemid J. Alloys and Compounds **485**, 642 (2009).
- [18] R. K Singh, Phys. Reports, **85**, 2592 (1982).
- [19] S. Singh, R.K. Singh, J. Phys. Soc. Jpn., **71**, 2477 (2002); R. K. Singh, S. P. Sanyal, Physica B **132**, 201 (1985); R.K. Singh, S. Singh, Phys. Rev. B **39**, 671 (1989), Phase Transit. **15**, 127 (1989).
- [20] K. N Jog, R. K Singh, S. P Sanyal, Phys. Rev. B **31**, 6047 (1985) .
- [21] S. Singh, Jour. Phys. Soc. Jpn., **71**, 70 (2002); S. Singh, R.K. Singh, High Pressure Research Jour. **21**(2), 105 (2001).
- [22] P.O. Lowdin, Ark. Mat. Astron. Fys., **35A**, 30 (1947); Adv. Phys. **5**, 1 (1956).
- [23] S O Lundqvist Ark. Fys. (Sweden), **12**, 365 (1957).
- [24] M P Tosi, F G Fumi J. Phys. Chem. Solids, **23**, 359 (1962) ; M P Tosi Solid State Physics **16**, 1 (1964) .
- [25] D W Hafemiester, H F Flygare, J. Chem. Phys. **43**, 795 (1965).
- [26] K Motida, J. Phys. Soc. Jpn., **55**, 1636 (1986).
- [27] P. Bhardwaj, S Singh, N. K. Gaur, J. of Molecular Structure: THEOCHEM, **897**, 95 (2009); P. Bhardwaj, S. Singh, N. K. Gaur, Mat. Res. Bull., **44**, 1366 (2009); P. Bhardwaj, S. Singh, N. K. Gaur, J. Cetr. Euro. J. Phys., **6**(2), 223 (2008).
- [28] R J Elliot and R A Leath, IIE 386 (1996).
- [29] L. Vegard, G. Scofteland, Arch. Math. Naturv. **45**, 163 (1942).
- [30] M. J. Mhel, R. J. Hemely, L. L. Boyer, Phys. Rev. B **33**, 8685 (1986).
- [31] H. Shimuzu, H. Tashiro, T. Kume, S. Sasaki, Phys. Rev. B **86**, 4568 (2001).
- [32] B B Karki, G J Ackland, J Crain, J. Phys.: Condens. Matter **9**, 8579 (1997).
- [33] T H K Barron, M L Klein, Proc. Phys. Soc., **85**, 523 (1965).
- [34] C S Zha, H K Mao, R J Hemley Proc. Natl Acad. Sci. USA, **97**, 13494 (2000).
- [35] G V Sin'ko, N A Smirnov J. Phys.: Condens. Matter, **14**, 69896 (2002); J. Phys.: Condense. Matter, **20**, 115203 (2008).
- [36] E Schreiber, O L Anderson, N Soga Elastic Constants and Their Measurements (New York: McGraw-Hill), 1973.

---

\*Corresponding author: purveebhardwaj@gmail.com